





Article

Shoreline Evolution and Environmental Changes at the NW Area of the Gulf of Gela (Sicily, Italy)

Laura Borzi ^{1,*} , Giorgio Anfuso ² , Giorgio Manno ³ , Salvatore Distefano ¹, Salvatore Urso ¹, Domenico Chiarella ⁴  and Agata Di Stefano ¹

¹ Department of Biological, Geological and Environmental Sciences, University of Catania, Corso Italia, 57, 95129 Catania, Italy; salvodist82@unict.it (S.D.); salvatore.urso@unict.it (S.U.); agata.distefano@unict.it (A.D.S.)

² Department of Earth Sciences, Faculty of Marine and Environmental Sciences, University of Cádiz, Polígono del Río San Pedro s/n, 11510 Puerto Real, Spain; giorgio.anfuso@uca.es

³ Department of Engineering, University of Palermo, Viale delle Scienze, Bd. 8, 90128 Palermo, Italy; giorgio.manno@unipa.it

⁴ Clastic Sedimentology Investigation (CSI), Department of Earth Sciences, Royal Holloway, University of London, Egham TW20 0EX, UK; Domenico.Chiarella@rhul.ac.uk

* Correspondence: laura.borzi@unict.it

Abstract: Coastal areas are among the most biologically productive, dynamic and valued ecosystems on Earth. They are subject to changes that greatly vary in scale, time and duration and to additional pressures resulting from anthropogenic activities. The aim of this work was to investigate the shoreline evolution and the main environmental changes of the coastal stretch between the towns of Licata and Gela (in the Gulf of Gela, Sicily, Italy). The methodology used in this work included the analysis of: (i) shoreline changes over the long- and medium-term periods (1955–2019 and 1989–2019, respectively), (ii) dune system fragmentation and (iii) the impact of coastal structures (harbours and breakwaters) on coastal evolution. The shoreline change analysis mainly showed a negative trend both over the long- and medium-term periods, with a maximum retreat of 3.87 m/year detected over the medium-term period down-drift of the Licata harbour. However, a few kilometres eastward from the harbour, significant accretion was registered where a set of breakwaters was emplaced. The Shoreline Change Envelope (SCE) showed that the main depositional phenomena occurred during the decade between 1955 and 1966, whereas progressive and constant erosion was observed between 1966 and 1989 in response to the increasing coastal armouring.

Keywords: shoreline changes; DSAS; dune fragmentation; coastal armouring



Citation: Borzi, L.; Anfuso, G.; Manno, G.; Distefano, S.; Urso, S.; Chiarella, D.; Di Stefano, A. Shoreline Evolution and Environmental Changes at the NW Area of the Gulf of Gela (Sicily, Italy). *Land* **2021**, *10*, 1034. <https://doi.org/10.3390/land10101034>

Academic Editor: Le Yu

Received: 10 September 2021

Accepted: 28 September 2021

Published: 2 October 2021

Publisher's Note: MDPI stays neutral with regard to jurisdictional claims in published maps and institutional affiliations.



Copyright: © 2021 by the authors. Licensee MDPI, Basel, Switzerland. This article is an open access article distributed under the terms and conditions of the Creative Commons Attribution (CC BY) license (<https://creativecommons.org/licenses/by/4.0/>).

1. Introduction

Natural coastal landscape modelling is an interactive complex phenomenon ruled by several dynamic processes, all linked in a non-linear way. Shorelines are dynamic in nature, and coastal behaviour is the result of natural and anthropic processes occurring and interacting on a variety of time and spatial scales [1–3]. The coastal sediment budget can be altered both by such physical processes, including waves, currents, tides, storm surges, seasonal fluctuations, aeolian transport and relative changes in sea level and by human actuations, such as the construction of inland infrastructure (e.g., dams) and coastal structures (e.g., protection structures and ports/harbours) [4]. However, decreased sediment river load and altered longshore drift appear to be pivotal factors in sediment coastal changes, and therefore manmade actuations can be the main causes of coastal erosion [5,6].

Most of the world's major cities are in coastal regions, and 40% of all people on the planet live within 100 km of a coastal zone [5]. Coastal settlements are often planned with insufficient attention to natural hazards such as coastal erosion and flooding, and often

coastal structures built too close to eroding shorelines experience wave inundation and damage [7,8]. In response, sea walls and revetments are often built to protect coastal homes, hotels and infrastructure, but their emplacement can lead to the total loss of the existing beaches [8].

As a result, numerous shoreline studies aim to quantify trends in shoreline change [8–13]. Shoreline studies are thus vital to the early stages of the decision-making process for planned coastal developments to mitigate the potential loss of buildings and infrastructure as well as to preserve natural environments such as beaches and dunes [14,15].

However, shoreline evolution studies can be challenging, and the computation of the rates of change should consider the processes that have affected the coast over time [16]. Nowadays different and varied cartographic datasets (i.e., aerial photographs, orthophotos, satellite imagery) provide useful tools to assess shoreline changes over the past decades, but the chosen spatial and temporal scales must be planned in advance to enhance the reliability of the data analysis. Indeed, long-term data (>60 years) produce more predictable trends, filtering out variations ranging from days to seasons typical of short-term fluctuations (<10 years) [16,17]. Consistency of the dataset and reliability of shoreline change analysis should be the basis of forecasting future shoreline position and wisely planning construction setbacks, especially in those areas of increasing economic growth [18].

About 20,000 km of coast, corresponding to 20% of the whole European coast length, faced serious impacts in 2004, and 15,100 km were actively retreating at the time, some of them despite the emplacement of coastal protection works [19]. Sicily (Southern Italy) is one of the regions with the highest coastal urban development in Europe, and about 900,000 inhabitants live within that area; more than 27% of the Sicilian coast has been still experiencing erosional phenomena, and more than 110 km of the coast have been armoured [19].

This paper represents the first analysis of the coastal evolution of one of the most human-impacted areas of Southern Sicily, i.e., the Gulf of Gela. This coast is highly valued because of its recreational, ecological, economic and cultural aspects, which strongly depend on its good status [20]. Therefore, investigation of local and regional coastal changes is of high priority for local managers to adopt sound management strategies to counteract erosion problems essentially related to inland human actions and the emplacement of hard protection structures on the coast. Thus, shoreline migration in response to the coastal and inland changes was studied. Rate-of-change statistics were computed on long- and medium-term periods by means of the ESRI ArcGIS® Digital Shoreline Analysis System (DSAS), and coastal environmental variations were quantified using the coastal armouring index [21] and the new dune fragmentation index proposed for the first time by Molina et al. [5].

2. Study Area

The area investigated in this paper, located on the Southern coast of Sicily (Italy), plays a key role in the economic strategies of the regional management. The area includes long and wide sandy beaches that enhance the development of leisure activities and infrastructures; greenhouse-crop systems are quite widespread thanks to mild weather conditions; on the coast of the Gela town stands one of the largest petrol-chemical poles in Europe that has been recently converted into a biorefinery, and some of the coastal regional strategic infrastructures insist on this wide coastal sector. Such strategic economic activities and human settlements are significantly affected by coastal erosional phenomena [20,22–24]. Therefore it is mandatory to understand past and actual shoreline trends to adopt sound management strategies to preserve coastal ecosystems and economic activities.

At a local scale, the Southern coast of Sicily is identified as a coastal sub-cell of I order by the Regional Plan against Coastal Erosion [20]. This cell has been split into II- and III-order sub-cells, and, in this paper, the shoreline evolution and the environmental changes of the third-order coastal sub-cell no. 4.2.2 were studied. The coastal area under study has a total length of 24.96 km, and it was subdivided into two sectors: sector no.

1, from the Licata harbour to the Falconara Castle, and sector no. 2, from the Falconara Castle to the Gela harbour (Figure 1). Sector no. 1 is ca. 10 km long, and the main coastal human work insisting on it is the Licata harbour. The harbour, essentially devoted to fishing activities, is considered a strategic infrastructure for the local economy. It has been implemented several times since the 1940s, and last modifications were carried out in 1997. Sector no. 2 stretches between the Falconara Castle and the Gela harbour and is ca. 15 km long.

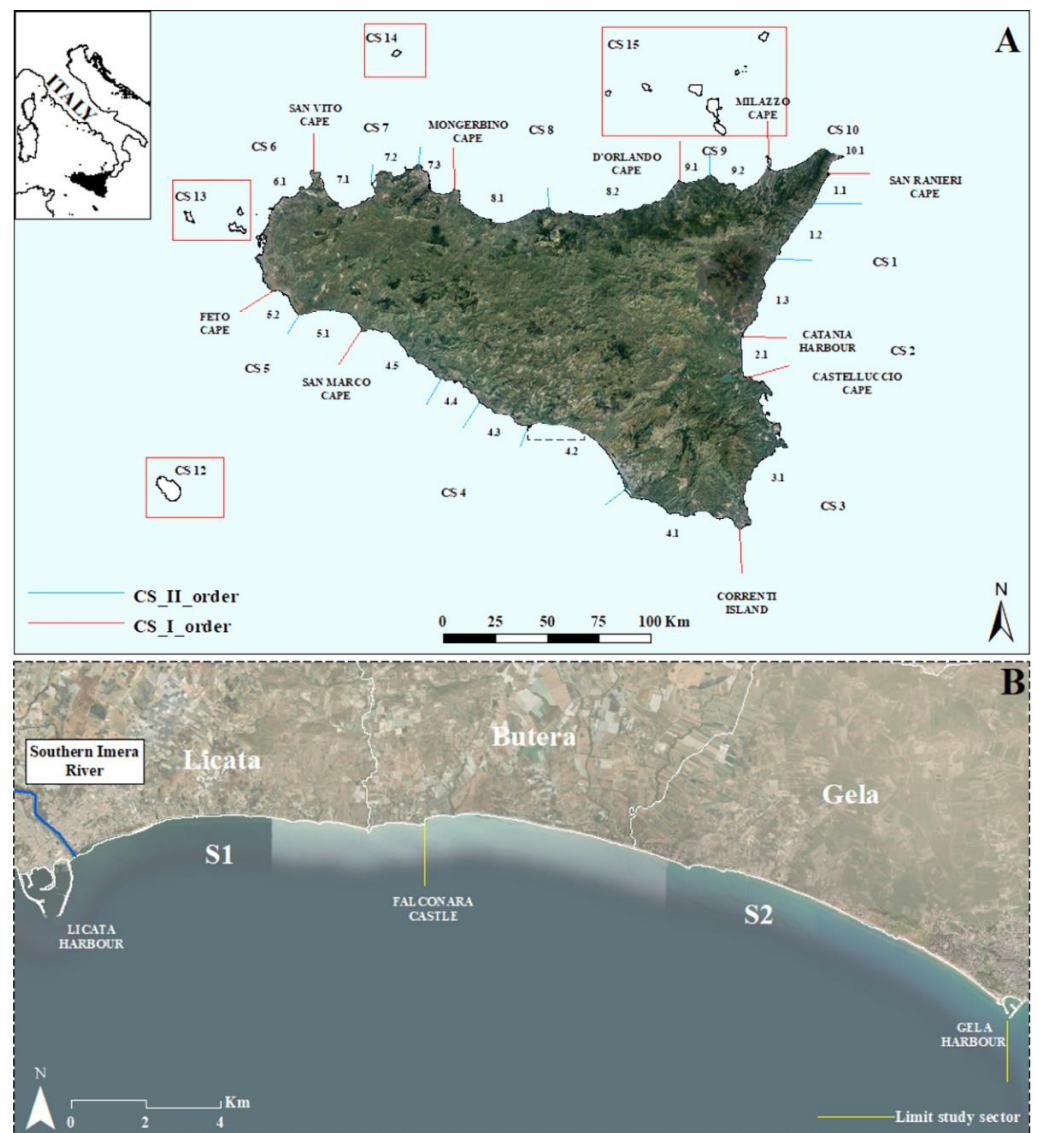


Figure 1. (A) The coastal sub-cell subdivision of Sicily in I- and II-order cells [20]; (B) The study area and its subdivision into two sectors: sector no. 1, from the Licata harbour to the Falconara Castle, and sector no. 2, from the Falconara Castle to the Gela harbour.

The Southern Imera River, set just a few metres east of the Licata harbour, is the main watercourse outflowing within the study area, and its drainage basin is the second largest one in Sicily (Figure 1) [25].

The river mouth profoundly changed during the past decades since it experienced significant lateral migration, and, consequently, the small harbour entrance has been repeatedly changed following the migration of the Southern Imera River mouth [23]. The lateral migration of the river mouth can be mainly related to the climatic modifications recorded between the 17th and 19th centuries and to the deforestation of the hinterland

deriving from the expansion of croplands [22]. Over the 1940s, the harbour was significantly expanded, and the first dikes (western and eastern) were emplaced.

The wind regime of the coastal area is dominated by winds blowing from the third quadrant and partly from the fourth quadrant, both in terms of frequency and maximum velocity [25,26]. The wave motion computed is mainly made of waves coming from the west-south-west, and the most energetic waves come from the west [27,28]. The area is characterized by a microtidal regime, as well-documented by the variations in levels at the tide gauge station located at Porto Empedocle (Figure 2).

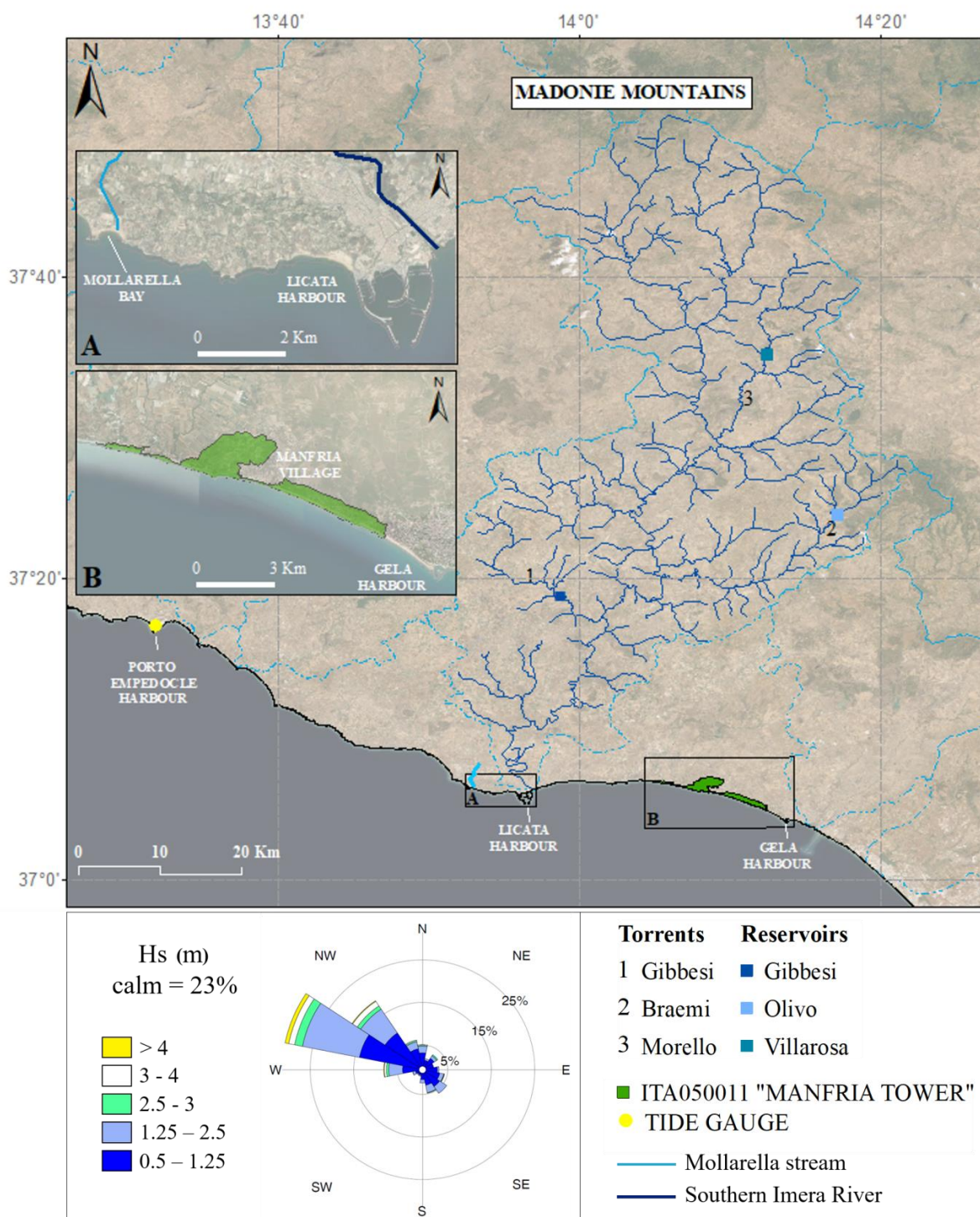


Figure 2. Southern Imera drainage basin, with tributaries and artificial reservoirs, location of the tide gauge station at Porto Empedocle (yellow dot) and the Site of Community Importance (SCI) ITA 050011 “Manfria Tower” (green polygon).

(A) Location of the present-day Southern Imera River mouth and the disused second river mouth, in correspondence of Mollarella Bay, ca. 6 km from the Licata harbour. (B) Details of the Site of Community Importance (SCI) ITA 050011 “Manfria Tower”.

The coast is essentially composed of narrow sandy beaches; a few headlands of small size are located east of the Falconara Castle promontory. Beach grain-size sediment ranges between fine and medium classes, and beaches generally show intermediate to dissipative morphodynamic states.

The Southern Imera crosses in the N–S direction the island of Sicily and until the early 1900s split into two streams just 5 km from the coastline [23]: the first outflowed in correspondence of the present mouth and the second towards the Mollarella Bay, 6 km westward of the Licata town, which was abandoned over the 1950s (Figure 2) [23]. Fluvial sediment inputs to the sub-cell are minimal, even though a high number of rivers and torrents flow out within this area; most of those rivers pass through predominantly chalk catchments, resulting in high solute but low sediment loads [23]. Three main artificial reservoirs intercept the Southern Imera River course: the Villarosa reservoir that blocks the Morello torrent, the Olivo reservoir, which blocks the Braemi torrent, and the Gibbesi reservoir, which is still not in operation. The Villarosa reservoir has been built nearby the town of Villarosa between 1969 and 1973, and it has a volume of 17.16 Mm³ and an estimated silting volume of 5.00×10^6 m³. In 1989, a bathymetric survey recorded an infilling volume of 1.37×10^6 m³. The Olivo reservoir has a total volume of 18 Mm³ and an estimated volume of 2.00×10^6 m³ [25] (Figure 2). One Natura 2000 site falls within the study area. Natura 2000 is an ecological network composed of sites designated under the Birds Directive (Special Protection Areas, SPAs) and the Habitats Directive (Sites of Community Importance, SCIs, and Special Areas of Conservation, SACs). The aim is to create breeding and resting sites for rare and threatened species and to protect some rare natural habitat types [29]. At 2 km eastward of the Falconara Castle, within sector no. 2, the Site of Community Importance ITA 050011 “Manfria Tower” is set; it is considered a biotope of high naturalistic and environmental interest, where a small dune ridge east of the Manfria Tower is still well preserved [30,31].

3. Materials and Methods

The main constraining factor for diachronic analysis is the availability of data for the specific study site [32]. The cartographic dataset covered a time span of 64 years, from 1955 to 2019. The data included (i) IGMI (Istituto Geografico Militare Italiano) aerial photographs (1955, 1966), (ii) orthophotographs (1989, 2000, 2006, 2012), available online at the website <http://www.pcn.minambiente.it/mattm> (accessed on 16 July 2021) [33], and (iii) Google images acquired by Google Earth (2016, 2019) [34]. Cartographic dataset resolution ranged from 0.5 m (Google Earth images) to 3 m (IGMI aerial photographs). Shorelines were acquired in ArcGIS 10.3 environment using as shoreline proxy the wet/dry line [32], and common coordinate system was set (Gauss–Boaga, Monte Mario Italy 2). The study area was split into two sectors limited by natural coastal physiographic or manmade structures. For each sector, the shoreline change analysis was carried out on medium-term period, covering a time span of 30 years (1989 to 2019) and on long-term period, between 1955 and 2019 [10]. The shoreline change analysis was based on the integration of remote sensing and geographic information system techniques. Shorelines were traced from aerial photographs, orthophotos and UAV image and analysed by the Digital Shoreline Analysis System (DSAS), which is an extension to ESRI ArcGIS© that can calculate the shoreline rate-of-change statistics starting from multiple historical shoreline positions [35]. The reliability of the statistics computed by the system mainly depends on the uncertainty value related to each shoreline dataset. In order to reduce the effect of short-term variability on long-term analysis, the uncertainties were considered independent, uncorrelated and

random, and, following [10,36–40], the total positional uncertainty of each dataset was calculated with the following equation:

$$\sigma_t = \sqrt{\sigma_d^2 + \sigma_p^2 + \sigma_r^2 + \sigma_{td}^2 + \sigma_{wr}^2} \quad (1)$$

The Digitizing Error (σ_d) was obtained detecting several times the same feature on the same image and calculating the error as the standard deviation of the residual value for that feature. The Pixel Error (σ_p) was assumed to be equal to the pixel size. For the Orthorectification Error (σ_r), the RMSE computed for the photogrammetric and polynomial rectification process was used as error value. The Tidal Fluctuation Error (σ_{td}) was considered as the variations in levels at the tide gauge station located at Porto Empedocle, 40 km NW from the study area. It is set in the harbour, and since 2010, the tide level is measured by a new sensor with millimetre accuracy, the SIAP+MICROS TLR. The min–max tidal range varied from 0.03 m to more than 1 m, but the average water level fluctuation was 0.04 m. The Weighted Linear Regression (WLR) rate index was classified following the methodology proposed by Molina et al. [12]. All values were normalized, and the Gaussian distribution was used to set the class limits (Table 1). More than 40% of all data ranged between ± 0.4 m, and it was assumed as the most recurrent smallest change due to seasonal oscillations and thus classified as stability state. Values between -0.4 and -0.7 m and between $+0.4$ and $+0.7$ m were considered as moderate erosion and moderate accretion, respectively, corresponding to 25% of all datasets; the remaining 34% data were grouped into 4 classes: high erosion (<-0.7 m; ≥ -1.5 m), very high erosion (<-1.5 m), high accretion (>0.7 m; ≤ 1.5 m) and very high accretion (>1.5 m). The percentage of each beach evolution class was computed for each sector.

Table 1. Beach evolution classes defined for the present work following the methodology proposed by Molina et al. [12].

Class	m/yr
Very high erosion	<-1.5
High erosion	$\geq -1.5; <-0.7$
Moderate erosion	$\geq -0.7; <-0.4$
Stability	$\geq -0.4; \leq +0.4$
Moderate accretion	$>+0.4; \leq +0.7$
High accretion	$>+0.7; \leq +1.5$
Very high accretion	$+1.5$

The coefficient of coastal armouring K [21] was used to assess the anthropogenic structure impact on the coastal area. It was computed dividing the total length of all emerged and visible submerged maritime structures (groins, moles, seawalls, revetments, breakwaters, etc.) by the entire length (L) of the coast under study, which was subdivided into subsectors of 500 m each. The extent of coastal armouring was “Minimal” at $K = 0.0001-0.1$, “Average” when $K = 0.11-0.5$, “Maximal” at $K = 0.51-1.0$ and “Extreme” if $K > 1.0$.

The dune fragmentation index (F) was proposed for the first time by Molina et al. [5]. It was used to assess how the dune systems have been impacted over time. The F index is expressed as the ratio between the length of all breaks (l) identified within a dune system and the whole dune toe length (L):

$$F = \frac{l}{L} \quad (2)$$

Each shorefront dune system was divided into 100 m sectors, and the F index was calculated for each. The F index can be grouped into three classes that were computed by us-

ing the Natural Breaks Function [5]. The annual level of dune fragmentation was computed as the average value for all sectors for each available photogrammetric flight. In the present paper, five classes were used to depict dune fragmentation evolution over time—limits between classes were calculated using the Natural Breaks Function applied to the total set of values obtained. Dune fragmentation level was “Null” ($F = 0$), “Low” ($0 < F \leq 0.05$), “Medium” ($0.05 < F \leq 0.1$), “High” and “Very High/Maximum” ($0.1 < F \leq 0.4$, $F > 0.4$, respectively).

4. Results

4.1. Shoreline Change Analysis

The long-term shoreline change analysis was carried out over a time span covering 64 years (1955–2019). Results show that within sector no. 1, covered by an amount of 380 transects (Figure 3), the area between the Licata harbour and the set of breakwaters (first 40 transects) registered very high erosion with a maximum WLR negative value of -6.25 m/year. The Southern Imera River mouth area has significantly eroded, and some buildings have been damaged by the intense shoreline landward movement (Figure 4).

The 1000 m of the coast, corresponding to the area protected by eleven breakwaters, experienced high (7%, 25 transects) to very high accretion (6%, 23 transects). A stable trend was recorded just down-drift of the breakwaters and along with 9.5 km (58% and 222 transects). The Net Shoreline Movement index registered a huge shoreline erosion between 1955 and 2019 close to the Southern Imera River mouth and a significant seaward movement where the Licata breakwaters are today set. The Shoreline Change Envelope index revealed that high accretional phenomena occurred between 1955 and 1966, but intensive erosional phenomena took place after 1966, even though they have been partly reduced by the trap action of the breakwaters.

Over the long-term time span, sector no. 2 experienced accretion that mainly occurred between the SCI “Manfria Tower” and the Gela harbour (Figure 5). In total, 37% of the data (205 transects) showed accretion, 32% recorded stability (181 transects), 13% of the coast faced moderate erosion (71 transects) and 18% high erosion (101 transects). The Net Shoreline Movement index registered the highest seaward migration east of the Licata harbour, and the Shoreline Change Envelope confirmed that accretion occurred over the 1955–2019 period.

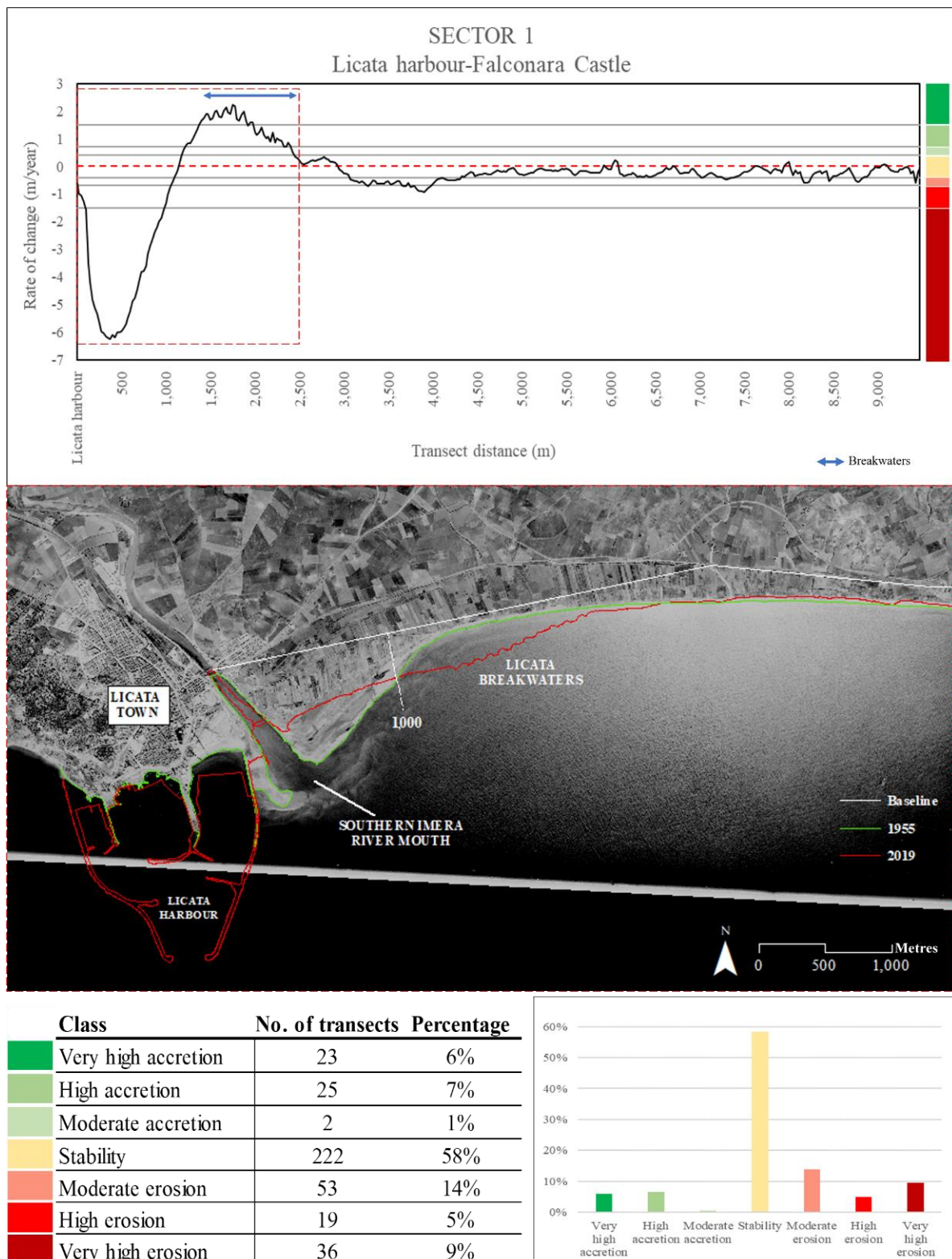


Figure 3. Rates of change within sector no. 1 over the long-term period (1955–2019). In total, 58% of the data falls within the stability state range, especially observed in the coastal area at a distance between 3 and 10 km from the harbour (highest negative WLR = -6.25 m/year), but significant sediment deposition was recorded between 1955 and 1989 where a set of breakwaters have been emplaced.

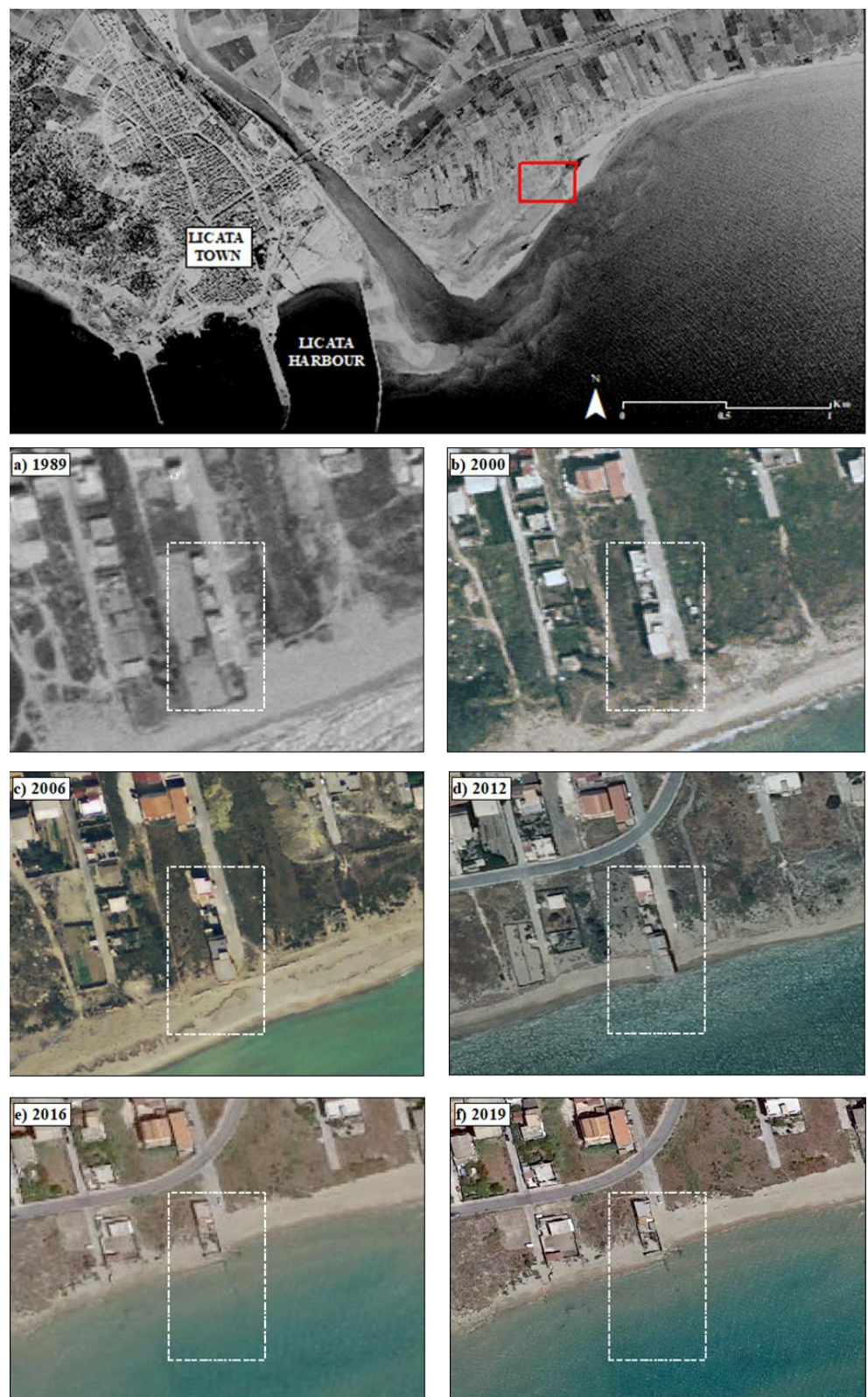


Figure 4. The area east of the Southern Imera River mouth faced severe coastal erosion. In 1955, the coastal area was undisturbed, but over the following decades, urbanization and anthropogenic disturbance have significantly increased, despite the severe erosion observed within this area, and (a–f) holidays houses have been seriously damaged and partly submerged, as shown by the white square that frames a house partly swallowed up by the sea.

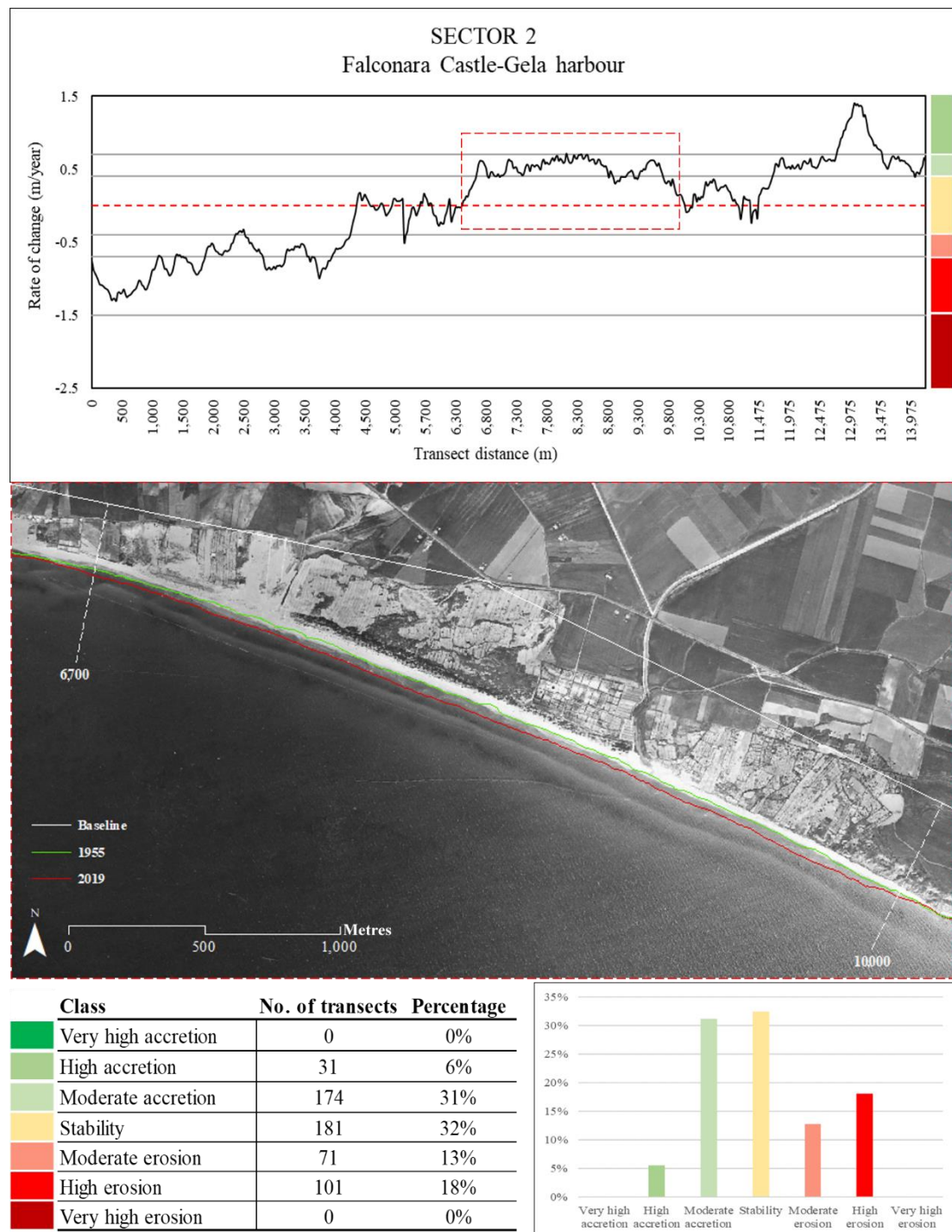


Figure 5. Shoreline evolution expressed as weighted linear regression rate within sector no. 2 over the long-term period (1955–2019). Stable trend (32%, 181 transects) was mainly recorded within sector no. 2, followed by moderate accretion (31%, 174 transects). Significant retreat occurred along 31% (172 transects) of the sector.

The medium-term shoreline change analysis was performed for the 1989–2019 time span. Within sector no. 1, 43% of the transects (165) fell within the stability state range, and erosion classes reached 48% (182 transects) with a maximum negative WLR value of 3.87 m/year registered nearby the Licata harbour. Lastly, the total accretion classes percentage was 9% (33 transects) and was only recorded at the set of breakwaters close to Licata (Figure 6).

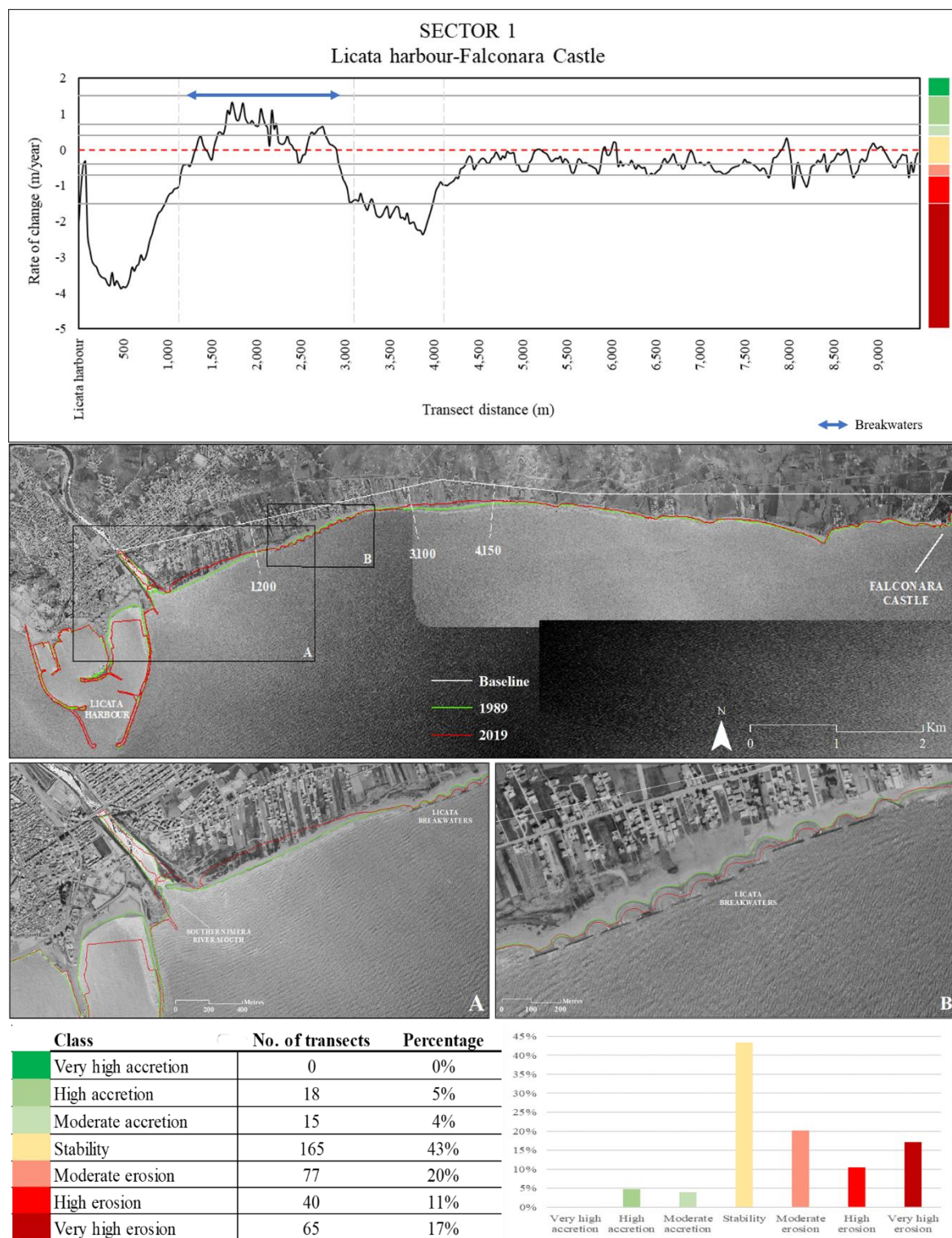


Figure 6. Shoreline changes over the mid-term period (1989–2019) within sector no. 1. Sector no. 1 is about 10 km long, from the Licata harbour to the Falconara Castle, but the rate-of-change plot indicated that the highest variability was detected within 4 km eastward of the Licata harbour. (A) The most severe erosion phenomena occurred right next to the Southern Imera River mouth; (B) accretional classes have been recorded about 1,2 km eastward the Licata harbour where 11 breakwaters have been emplaced to block the intense sediment loss.. Grey dashed lines are those transects cast by the DSAS and delimit coastal areas that have recorded main changes.

Within sector no. 2, stability state class represented 38% of the data (210 transects), even though most of the stable transect values were recorded at the eastern part of the coast, and moderate accretion values (18%) were mainly found along the coast falling within the Site of Community Importance “Manfria Tower”. Shoreline erosion was mostly observed at the western part of the sector, where the shoreline faced a maximum retreat of 1.73 m/year (Figure 7).

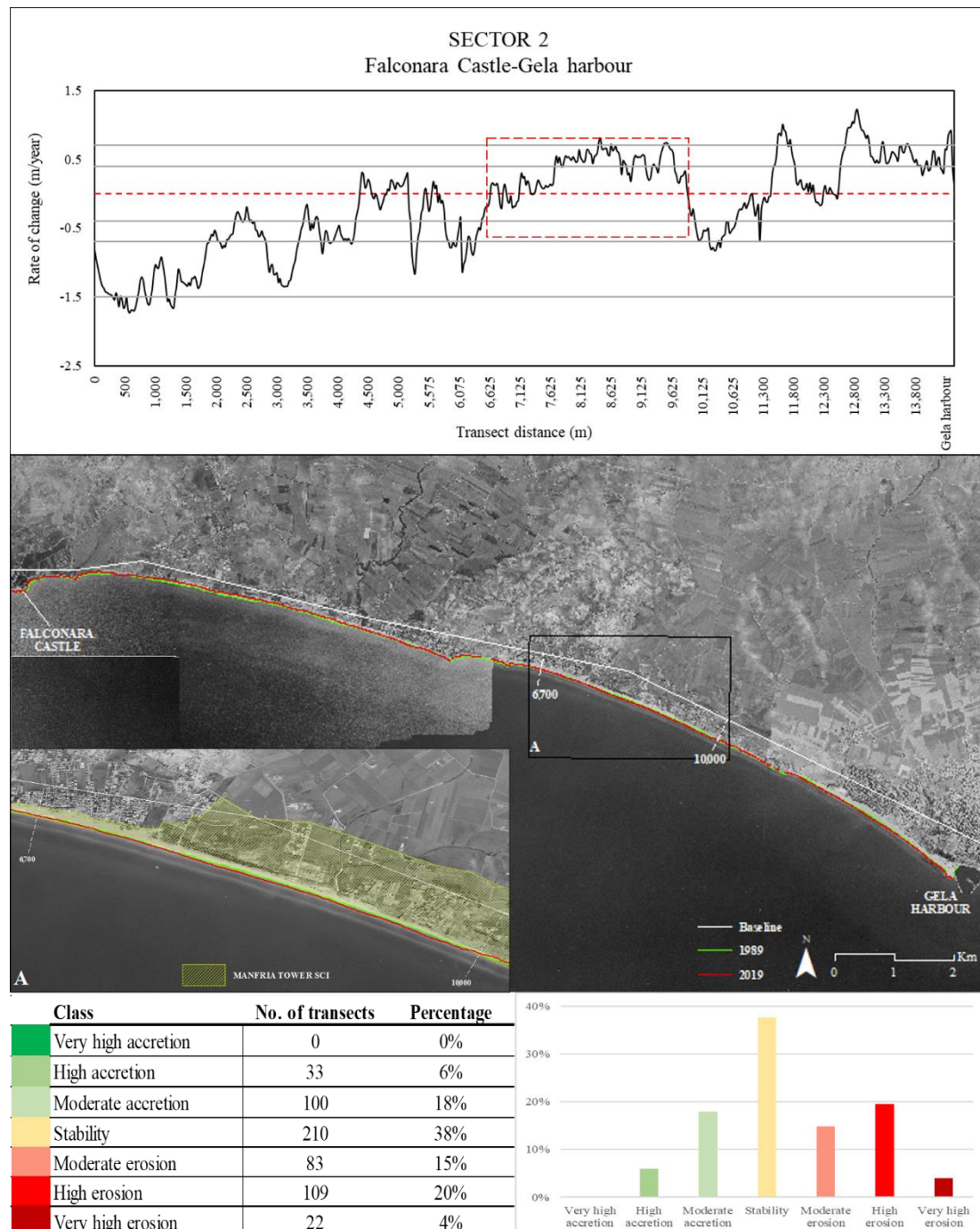


Figure 7. Shoreline evolution over the mid-term period (1989–2019) within sector no. 2. This sector mostly showed a stable trend (38%, 210 transects). In total, 39% of the coast faced moderate to very high erosion (214 transects), and 24% ranged between moderate and high accretion (133 transects). (A) Higher sediment deposition processes have been recorded in correspondence of the Site of Community Importance ITA 050011 – Manfria Tower. Grey dashed lines are the transects at 6350 m and at 10,125 m from the westernmost edge of the sector.

4.2. Dune Fragmentation Analysis

The dune system detected in the 1955 and 1966 aerial photographs presents a great alongshore continuity. Therefore, the dune fragmentation index computed for those years was null. Over time, continuity of dune system toe and associated vegetation line significantly decreased (Figure 8).

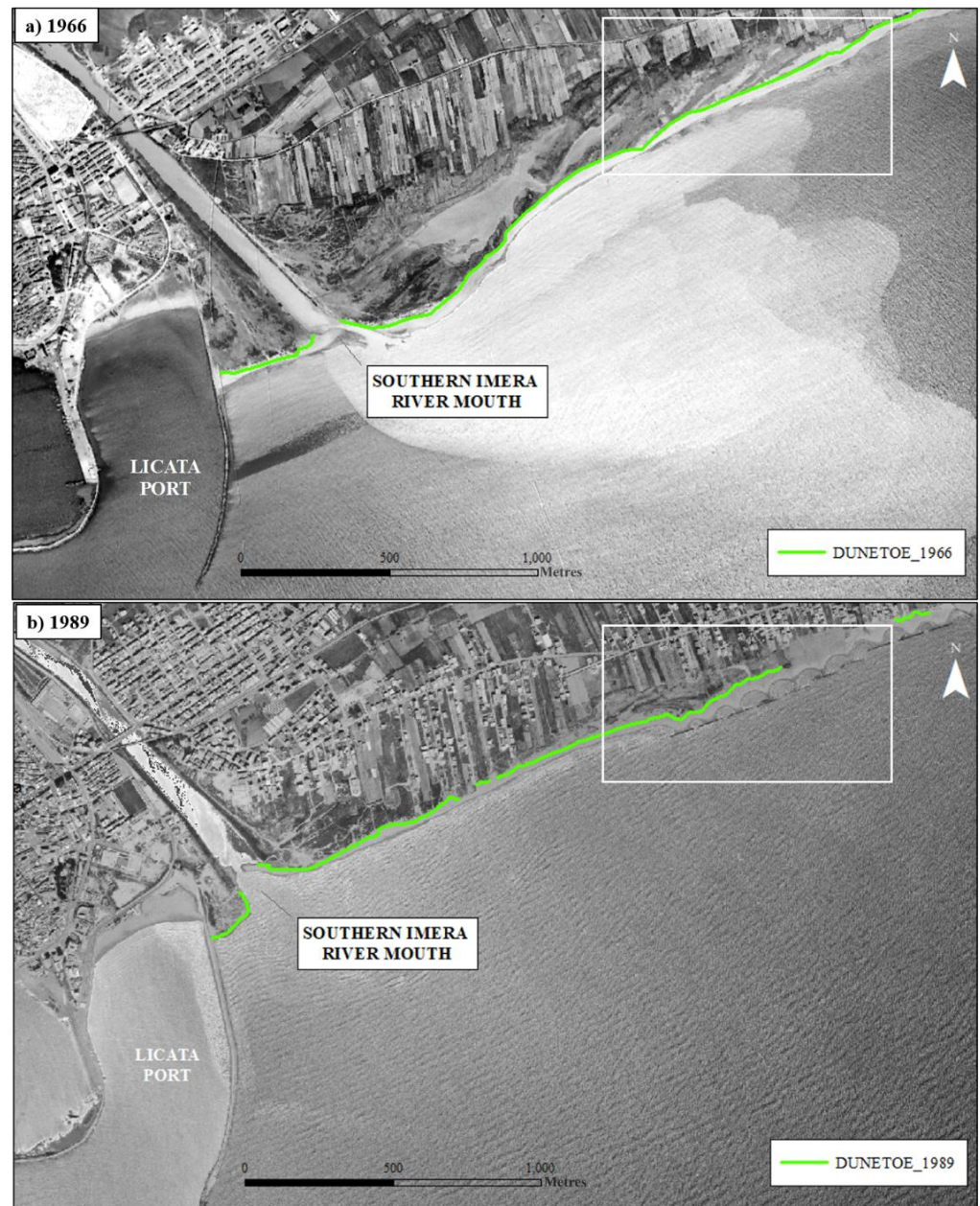


Figure 8. Dune toe detected nearby the Licata port on the 1966 aerial photo and on the 1989 orthophoto. (a) The dune system in 1966 is several kilometres long and only interrupted by physiographic or natural elements. (b) In 1989, the dune ridge significantly retreated (white square) and was partly interrupted by manmade works. Green line is the dune toe proxy.

Over the period between 1989 and 2019, nine dune systems were detected along the two sectors: two within sector no. 1 and seven within sector no. 2. The dune fragmentation index was computed for each system. Dune system no. 1 totally disappeared over the time span between 1989 and 2012 ($F = 1$ in 2012, “Very High/Maximum” class), but in 2016, dune system no. 1 was naturally recovered. Two of the nine systems experienced an increase

in dune fragmentation, and seven of them did not change their class. As such, 56% of the dune systems were not fragmented at all in 1989, and 22% were scarcely fragmented (“Low” fragmentation class). The tendency changed after 2006 when the “Very high/Maximum” class appeared for the first time. The “Medium” class varied as well from 0% in 1989 to 22% in 2016. In 2019, the “Very high/Maximum” class was not observed anymore; most of the dune system fragmentation values fell within the range of the “Null” and “Low” classes (55%, five dune systems), but 33% of the systems were still highly fragmented (Figure 9).

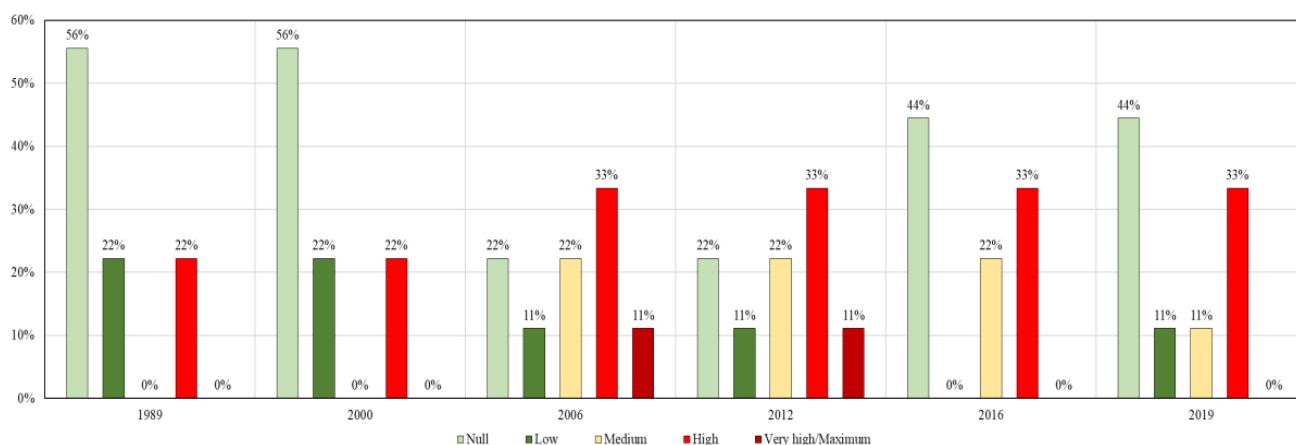


Figure 9. Percentage of F index classes per year. In 1989, the most frequent classes are the “Null” and the “Low” fragmentation ones, “Medium” fragmentation class is not represented at all, the “High” one is 21%, and the “Very High/Maximum” fragmentation class has not been found.

4.3. Coastal Armouring Analysis

The coefficient of coastal armouring (K) was computed to assess the maritime structures’ impact on the shoreline evolution. This coefficient represents the ratio between the total length of all maritime hydraulic structures (groins, seawalls, dikes, jetties, etc.) and total coastal length of the study area; the study area was, however, subdivided into subsectors of 500 m each [21].

Table 2 shows the coefficient of coastal armouring (K), the total coastal length (L) per year and the total length of coastal structures (I) per year. Over the 1950s and 1960s, the Licata harbour was the only infrastructure insisting on the coast. The K value computed for sector no. 1 did not appreciably vary over those years and fell within the “Maximal” range class (0.5–0.8). A few coastal structures were detected in 1955 and 1966 within sector no. 2. In 1989, the K value of sector no. 1 resulted to be significantly higher (1.2) reaching the “Extreme” class. Sector no. 2 did not register any change. Between 1966 and 1989, the total structure length significantly increased, mainly due to the Licata harbour implementation. Eleven breakwaters were built eastward of the Licata harbour over those decades. Over the 2000–2019 time span, the coefficient K slightly increased within sector no. 1, varying from 1.3 to 1.6 (i.e., “Extreme” class). Within sector no. 2, no changes were detected.

Table 2. The coefficient of coastal armouring K computed for each sector per year. The Total Coastal Length (L) and the Total Structure Length (I) per year are shown. All measures are expressed in metres (m). Sector no. 1 experienced significant increase, with K passing from “Maximal” (K = 1.2 in 1989) to the “Extreme” class (K = 1.6 in 2019). Sector no. 2 did not face any changes over the considered time span.

Year	Sector	Total Coastal Length (L)	Total Structure Length (I)	K
1955	1	9826	7706	0.8
1966	1	10,134	8443	0.8

Table 2. *Cont.*

Year	Sector	Total Coastal Length (L)	Total Structure Length (I)	K
1989	1	10,216	11,969	1.2
2000	1	10,198	13,640	1.3
2006	1	9727	13,918	1.4
2012	1	9732	15,014	1.5
2019	1	9719	15,456	1.6

5. Discussion

In the following sections, the shoreline changes along the two sectors are discussed as the main erosional/accretional/stable phenomena observed. The findings on the shoreline evolution are interpreted in the light of the main environmental coastal variations, considering the main river variations, the dune fragmentation level and the coastal armouring impact.

The mid- and long-term period analyses showed that the coastal area under study mainly experienced stability (43% and 58%, respectively). However, significant shoreline changes were observed within the area of the Southern Imera River mouth, and 9% of very high erosion phenomena were recorded down-drift of the Licata harbour, where the highest WLR negative value was also detected (-6.25 m/year). Amore et al. [23] showed that significant erosional phenomena were observed at the Southern Imera River mouth earlier than the 1960s, and coastal progradation was mainly observed over the past decades. The Shoreline Change Envelope index confirmed that high accretional phenomena occurred between 1955 and 1966, and the shoreline significantly began retreating after 1966 (Figure 10). As already shown by Amore et al. and Amore and Randazzo [23,41], the higher accretion rate detected over the decade 1950–1960 can be explained by the increasing river sediment load caused by (i) the disuse of the secondary stream mouth of the Southern Imera River and (ii) the deforestation of the drainage basin area to make space for crops and cultivation [23]. Deforestation is considered as a triggered event for coastal advancement, as shown by Pranzini [42] in the area of the Arno and Ombrone River deltas in Italy and by Zengcui and Zeheng [43] in the area of the Qiantang estuary in China. After the 1960s, the sediment supplies to the two studied sectors significantly decreased due to the implementation of (i) the Villarosa, Olivo and Gibbesi artificial reservoirs, which were built over the decade 1960–1970, and (ii) the Licata harbour. The reservoirs blocked the Southern Imera River course to satisfy the huge increase in irrigation water demands, forming sediment traps and reducing the peak flood flows, thereby decreasing the sediment supply to the coast. The decrease of sediment river discharge caused by the implementation of dams is a pivotal factor in beach retreating. Roskopf et al. [44] pointed out that the long-term shoreline retreat of the Molise coast (Italy) was primarily related to channel adjustments of the Biferno and Trigno rivers, trapping most of the rivers' solid load, affecting the sediment budget of the river mouth areas and adjacent beaches. The reduction in sediment discharge caused by the dams was also well studied by Amrouni et al. [13], who considered the implementation of artificial reservoirs as the main cause of the negative sediment budget leading to a shortage of sand sediment on the Medjerda delta (Tunisia) and the dominant erosion of the coastline. The reduced flux of sediment reaching the world's coasts because of retention within reservoirs is also well documented by Syvitski et al. [45], who estimated that over 100 billion metric tons of sediment are sequestered in reservoirs constructed largely within the past 50 years.

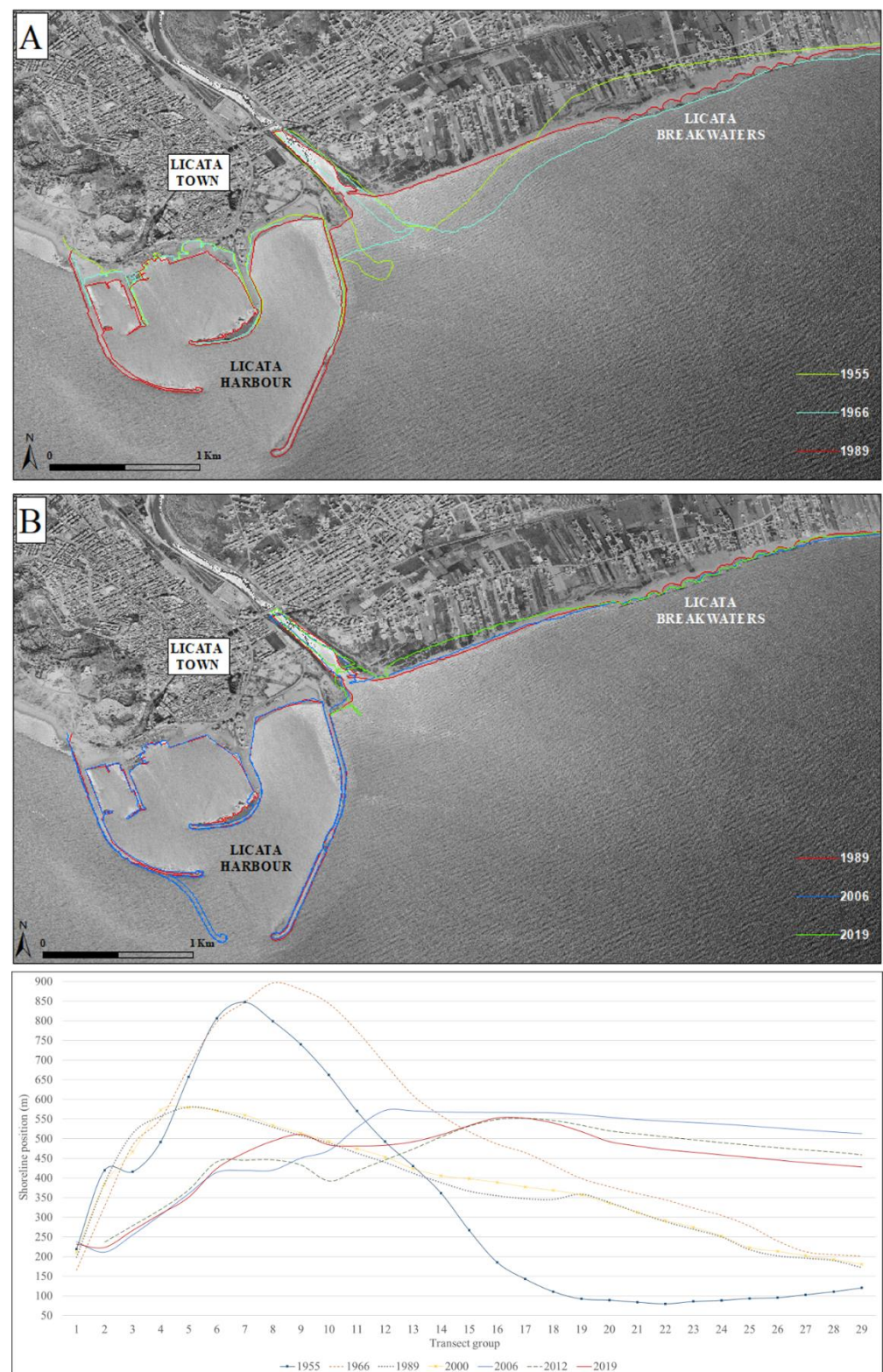


Figure 10. The shoreline evolution of the Southern Imera River mouth and the area east of the mouth. The trend seemed to be negative between 1955 and 2016, but the Shoreline Change Envelope revealed that (A) significant accretion has been recorded between 1955 and 1966, and very high erosion has been registered between 1966 and 1989, as shown by the interpolated plot of the shoreline changes (1 transect group = 100 m), but (B) shoreline moved seaward between 1989 and 2016 where a set of eleven breakwaters was emplaced.

Over the time between 1955 and 2019, the coastal area between Licata and Gela has been modified following the increasing economic growth that occurred after the Second World War. Between the 19th and the 20th centuries, the town of Licata became one of the biggest industrial centres in Europe for the refinement of sulphur which led to the implementation of a larger harbour accessible for larger ships served by a railway line [23]. As a result, (i) the harbour impounded littoral material, partly interrupting the W–E longshore sediment load [12,46,47], and (ii) the dune systems of the area nearby the Licata town have been profoundly damaged due to the increase in urbanization, as largely observed worldwide in areas of rapid economic growth [48–53].

However, the highest retreats were also recorded down-drift of coastal structures (harbours and breakwaters), and sediment deposition was mainly found in correspondence of structures (i.e., breakwaters) and along coastal areas where beaches are backed by well-preserved dune systems and breakwater barriers (Figure 11). Indeed, east of the Licata harbour, a set of eleven breakwaters was emplaced to face the huge landward migration of the Southern Imera River mouth and of the proximal coastal area. Moderate to high erosion phenomena were observed down-drift of the set of structures, whereas accretion was recorded in correspondence and up-drift of them, with a maximum value of 2.22 m/year (Figure 11). The same trend, i.e., significant accretion, was observed within sector no. 2, up-drift of two breakwaters emplaced westward of the Gela harbour. A few kilometres westward of the study area, at San Leone beach, Manno and Ciraolo [54] showed that the maritime works (port, groins and breakwaters), which were emplaced to limit the increasing shoreline retreat, changed the original coastal equilibrium, affecting the coastal sediment transport and thus causing very high variability in shoreline position up-drift and down-drift of the coastal structures. In nearby South-eastern Sicilian areas, Anfuso et al. [55] confirmed as well the common tendency of accretion/erosion at up-drift/down-drift of coastal structures, respectively. Coastline armouring is a very common engineering solution against erosion [46,56], but there are a number of adverse influences, including disturbance of cross- and long-shore sediment transport, associated with up-drift sedimentation but down-drift beach reduction, accelerated bottom erosion in front of structures, restricted public access to the beach, formation of dangerous currents for bathers and negative impact on landscape value [8,46,57–61]. Worldwide examples of anthropogenic disturbance (i.e., coastal armouring) on the coastal dynamic are well documented. Sousa et al. [61,62] showed that coastal structures are the most applied short-term solutions to coastal erosion in Massaguaçu Beach (Brazil) but not the most efficient ones, often changing the long-shore transport, affecting the beach profile and the scenic beauty of the beach, and thus increasing coastal vulnerability.

Moderate to high accretion classes were recorded in correspondence of the Site of Community Importance ITA 050011 “Manfria Tower”, where the long and wide beach is backed by a well-preserved dune ridge. Such accretion processes have been probably active for several decades as it is reflected by the formation of such well-developed dune systems. Within sector no. 2, the coastal land use has not significantly changed over time, and the area did not face huge coastal changes both in terms of dune fragmentation and of implementation of coastal structures. The Site of Community Importance ITA 050011 “Manfria Tower” acted as a constraining factor to human pressure on this area. As observed in Australia, at places, recent human disturbance is the main cause of the increasing sediment supply to dune systems, often resulting in foredune formation [63]. Moreover, natural dunes often provide sediment reservoirs to the shore and act as barriers to erosion and flooding processes, as showed by Manca et al. [64] in West Sardinia (Italy), where the dune system at Maria Pia beach is still acting as a source of sand. Saye et al. [65] in the UK demonstrated that dune morphology often reflects beach morphology (width, slope, sediment grain size, etc.); indeed, high foredune ridges develop where the sediment budget of the beach and dune is in balance. However, Saye et al. [65] also found that, within an accreting coastal sector, new dune ridges can progressively form, and the maximum crest height of each ridge is limited by the rate of beach accretion and shoreline progradation.

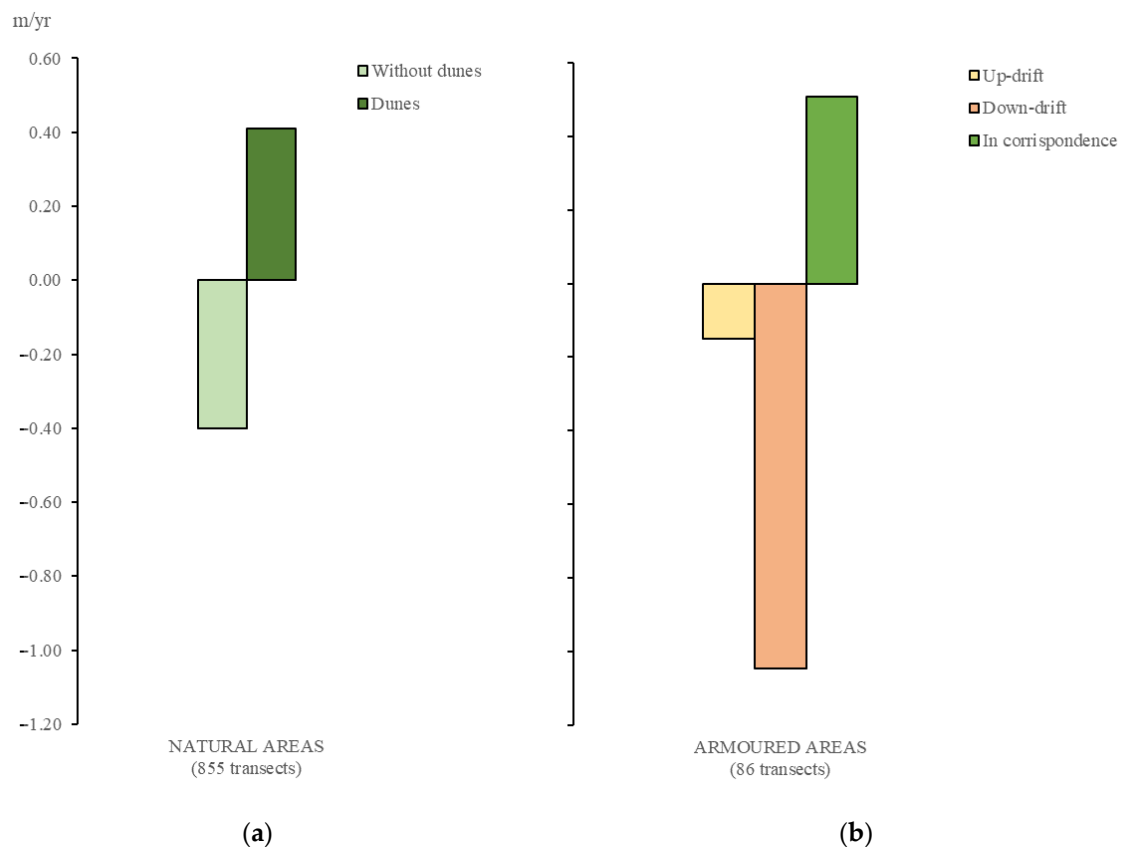


Figure 11. Shoreline evolution plot of the average WLR values found in correspondence of transects placed at (a) natural areas, subdivided into areas backed by dunes (93 transects) and areas without dunes (762 transects), and at (b) armoured areas, considering the up-drift and down-drift zones and in correspondence of structures (48 transects).

6. Conclusions

The shoreline evolution and the environmental changes of the coastal strip between the Licata harbour and the Gela harbour (Southern Sicily, Italy) were investigated over mid- and long-term periods (1989–2019 and 1955–2019, respectively). This study showed that (i) significant shoreline retreat occurred in correspondence of the Southern Imera River mouth, where, on one hand, the construction of artificial reservoirs along the river course caused the shortage of sediment river discharge and, on the other hand, coastal environmental changes, as the progressive implementation of the Licata harbour and the significant loss of the dune ecosystem, altered the coastal sediment dynamic; (ii) coastal armoured affected longshore sediment transport, giving rise to sediment deposition in correspondence and up-drift of structures (i.e., breakwaters), while relevant retreat is generally found down-drift of coastal structures (harbours and breakwaters); and (iii) beaches backed by a well-preserved dune system experienced sedimentation or maintained a stable trend as dunes likely provide sediment reservoirs to the shore and act as barriers to erosion and flooding processes.

The lack of coastal management strategies and non-integrated decision-making processes often triggered an increase in coastal zone vulnerability. Within sector no. 1, despite the severe erosional phenomena recorded, improper land-use planning has been carried out and buildings have been seriously damaged and progressively destroyed by wave processes. As such, this study can be the starting point to forecast future shoreline trends (taking also into consideration climate change processes) and can support the local coastal management administrations to properly plan sustainable policies in a long-term scenario, i.e., assess areas at high risk of erosion and flooding, evaluate the efficiency of coastal

armouring and of natural protected coastal sectors and identify best resilience solutions to stabilise and limit the impacts related to coastal erosion.

Author Contributions: Conceptualization, L.B., A.D.S. and D.C.; Methodology, L.B., G.A., G.M., A.D.S. and D.C.; Software, L.B., G.M. and G.A.; Formal analysis, L.B., A.D.S., D.C., G.A., G.M., S.D. and S.U.; Data curation, L.B., A.D.S., D.C., G.A., G.M., S.D. and S.U.; writing—original draft preparation, L.B., A.D.S., D.C., G.A., G.M., S.D. and S.U.; writing—review and editing, A.D.S., D.C., G.A., G.M., S.D. and S.U. All authors have read and agreed to the published version of the manuscript.

Funding: The study also benefited from grants assigned in the framework of the Project n. 183371—CUP E66C18001300007 “Attraction and International Mobility” (AIM) funded by the Italian MIUR (Ministry of Instruction and University and Research) (D.D. 407/27.2.2018) Action 1.2 Axis I-PON R&I 2014–2020 Blue Growth Area (Beneficiary: Salvatore Distefano; Scientific Responsible: Agata Di Stefano).

Informed Consent Statement: Not applicable.

Data Availability Statement: Not applicable.

Acknowledgments: Special thanks go to Giuseppe Ciraolo and Carlo Lo Re for the support given on the uncertainties and errors computation.

Conflicts of Interest: The authors declare no conflict of interest.

References

- Bird, E.C.F. *Submerging Coasts: The Effects of a Rising Sea Level on Coastal Environments*; Wiley and Sons: New York, NY, USA, 1993; p. 184.
- Pethick, J. Coastal management and sea-level rise. *Catena* **2001**, *42*, 307–322. [\[CrossRef\]](#)
- Todd, P.A.; Heery, E.C.; Loke, L.H.; Thurstan, R.H.; Kotze, D.J.; Swan, C. Towards an urban marine ecology: Characterizing the drivers, patterns and processes of marine ecosystems in coastal cities. *Oikos* **2019**, *128*, 1215–1242. [\[CrossRef\]](#)
- Komar, P.D. *Beach Processes and Sedimentation*, 2nd ed.; Prentice Hall: Upper Saddle River, NJ, USA, 1998; p. 544.
- Molina, R.; Manno, G.; Re, C.L.; Anfuso, G. Dune systems’ characterization and evolution in the Andalusia Mediterranean Coast (Spain). *Water* **2020**, *12*, 2094. [\[CrossRef\]](#)
- Di Stefano, A.; De Pietro, R.; Monaco, C.; Zanini, A. Anthropogenic influence on coastal evolution: A case history from the Catania Gulf shoreline (eastern Sicily, Italy). *Ocean. Coast. Manag.* **2013**, *80*, 133–148. [\[CrossRef\]](#)
- Wong, P.P.; Losada, I.J.; Gattuso, J.-P.; Hinkel, J.; Khattabi, A.; McInnes, K.L.; Saito, Y.; Sallenger, A.; Cheong, S.-M.; Dow, K.; et al. Coastal systems and low-lying areas. In *Climate Change 2007: Impacts, Adaptation and Vulnerability. Contribution of Working Group II to the Fourth Assessment Report of the Intergovernmental Panel on Climate Change*; Nicholls, R.J., Santos, F., Eds.; Cambridge University Press: Cambridge, UK, 2007; pp. 315–356.
- European Environmental Agency. *The Changing Faces of Europe’s Coastal Areas*; Office for Official Publications of the European Communities: Bruxelles, Belgium, 2006.
- Romine, B.M.; Fletcher, C.H. Armoring on eroding coasts leads to beach narrowing and loss on Oahu, Hawaii. In *Pitfalls of Shoreline Stabilization*; Springer: Dordrecht, The Netherlands, 2012; pp. 141–164.
- Crowell, M.; Leatherman, S.P.; Buckley, M.K. Historical shoreline change: Error analysis and mapping accuracy. *J. Coast. Res.* **1991**, *7*, 839–852.
- Galgano, F.A.; Douglas, B.C.; Leatherman, S.P. Trends and variability of shoreline position. *J. Coast. Res.* **1998**, *26*, 282–291.
- Molina, R.; Anfuso, G.; Manno, G.; Gracia Prieto, F.J. The Mediterranean coast of Andalusia (Spain): Medium-term evolution and impacts of coastal structures. *Sustainability* **2019**, *11*, 3539. [\[CrossRef\]](#)
- Amrouni, O.; Sánchez, A.; Khélifi, N.; Benmoussa, T.; Chiarella, D.; Mahé, G.; Abdeljaouad, S.; & McLare, P. Sensitivity assessment of the deltaic coast of Medjerda based on fine-grained sediment dynamics, Gulf of Tunis, Western Mediterranean. *J. Coast. Conserv.* **2019**, *23*, 571–587. [\[CrossRef\]](#)
- Coelho, C.; Silva, R.; Veloso-Gomes, F.; Taveira Pinto, F. A vulnerability analysis approach for the Portuguese west coast. In *Risk Analysis V: Simulation and Hazard Mitigation*; Popov, V., Brebbia, C.A., Eds.; WIT Press: Southampton, UK, 2006; pp. 251–262.
- Anfuso, G.; Martínez Del Pozo, J.Á. Assessment of coastal vulnerability through the use of GIS tools in South Sicily (Italy). *Environ. Manag.* **2009**, *43*, 533–545. [\[CrossRef\]](#) [\[PubMed\]](#)
- Dolan, R.; Fenster, M.S.; Holme, S.J. Temporal analysis of shoreline recession and accretion. *J. Coast. Res.* **1991**, *7*, 723–744.
- Crowell, M.; Leatherman, S.P.; Buckley, M.K. Shoreline change rate analysis: Long term versus short term data. *Shore Beach* **1993**, *61*, 13–20.
- Molina, R.; Manno, G.; Re, C.L.; Anfuso, G.; Ciraolo, G. A Methodological approach to determine sound response modalities to coastal erosion processes in mediterranean andalusia (Spain). *JMSE* **2020**, *8*, 154. [\[CrossRef\]](#)

19. Salman, A.; Lombardo, S.; Doody, P. *Living with Coastal Erosion in Europe: Sediment and Space for Sustainability*; Hydraulic Engineering Reports; EuroSION project; EUCC: Porto, Portugal, 2004; p. 21.
20. Sicilian Region—Office of the Commissioner of Government against the Hydrogeological Instability in the Sicilian Region. In *Regional Plan against Coastal Erosion 2020*; v. 1.0; Sicilian Region—Office of the Commissioner of Government: Sicily, Italy, 2020; p. 1527.
21. Aybulatov, N.A.; Artyukhin, Y.V. *Geo-Ecology of the World Ocean's Shelf and Coasts*; Hydrometeo Publishing: Saint Petersburg, Russia, 1993; p. 304.
22. Brambati, A.; Amore, C.; Giuffrida, E.; Randazzo, G. Relationship between the port structures and coastal dynamics in the Gulf of Gela (Sicily-Italy). In *Proceedings of the International Coastal Congress ICC*, Kiel, Germany, 6–13 September 1992; pp. 773–793.
23. Amore, C.; Geremia, F.; Randazzo, G. Historical evolution of the Salso River mouth with respect to the Licata harbour system (Southern Sicily, Italy). In *Littoral The Changing Coast*; EUROCOAST/EUCC: Porto, Portugal, 2002; pp. 253–260.
24. Martino, C.; Curcuruto, E.; Di Stefano, A.; Monaco, C.; Zanini, A. Fenomeni erosivi lungo il litorale di Marina di Butera (CL), Sicilia centro-meridionale. *Geol. Di Sicil.* **2011**, *3*, 4–15.
25. Regione Siciliana—Assessorato Territorio e Ambiente—Dipartimento Territorio e Ambiente. Servizio III Assetto del Territorio e Difesa del Suolo. Piano Stralcio di Bacino per l'Assetto Idrogeologico della Regione Siciliana; (P.A.I.). Bacino Idrografico del F. Imera Meridionale (072) Area territoriale tra il Bacino Idrografico del F. Palma e il Bacino Idrografico del F. Imera Meridionale (071). 2008. Available online: <https://www.sitr.regione.sicilia.it/pai/bacini.htm> (accessed on 30 September 2021).
26. Anfuso, G.; Martínez del Pozo, J.Á.; Rangel-Buitrago, N. Bad practice in erosion management: The southern Sicily case study. In *Pitfalls of Shoreline Stabilization: Selected Case Studies*; Cooper, J.A.G., Pilkey, O.H., Eds.; Springer: Berlin/Heidelberg, Germany, 2012; Volume 3, pp. 215–233.
27. Regione Siciliana—Assessorato Territorio e Ambiente, Dipartimento Territorio e Ambiente. Servizio 4, Assetto del territorio e difesa del suolo. Piano Stralcio di Bacino per l'Assetto Idrogeologico; (P.A.I.). UNITA' FISIOGRAFICA N° 8—PUNTA BRACCETTO—PORTO DI LICATA. 2007. Available online: <https://www.sitr.regione.sicilia.it/pai/unitafisiografiche.htm> (accessed on 30 September 2021).
28. Foti, E.; Musumeci, R.E.; Leanza, S.; Cavallaro, L. Feasibility of an offshore wind farm in the gulf of Gela: Marine and structural issues. *Wind. Eng.* **2010**, *34*, 65–84. [\[CrossRef\]](#)
29. European Commission. Available online: http://ec.europa.eu/environment/nature/legislation/habitatsdirective/index_en.htm (accessed on 24 March 2020).
30. Brullo, S.; Minissale, P.; Spampinato, G. Considerazioni fitogeografiche sulla flora della Sicilia. *Ecol. Mediterr.* **1995**, *21*, 99–117. [\[CrossRef\]](#)
31. Giusso Del Galdo, G.; Sciandrello, S. Contributo alla flora dei dintorni di Gela (Sicilia meridionale). In *98° Congresso della Società Botanica Italiana, Riassunti*; Università di Catania: Catania, Italy, 2003; p. 235.
32. Boak, E.H.; Turner, I.L. Shoreline definition and detection: A review. *J. Coast. Res.* **2005**, *21*, 688–703. [\[CrossRef\]](#)
33. Geoportale Nazionale. Available online: <http://www.pcn.minambiente.it/mattm> (accessed on 16 July 2021).
34. Google Earth. Available online: <https://earth.google.com/web> (accessed on 16 July 2021).
35. Thieler, E.R.; Himmelstoss, E.A.; Zichichi, J.L.; Ergul, A. *Digital Shoreline Analysis System (DSAS) version 4.0—An ArcGIS Extension for Calculating Shoreline Change*; U.S.G.S. Open-File Report; U.S. Geological Survey: Reston, VA, USA, 2008; Volume 1278.
36. Manno, G.; Lo Re, C.; Ciraolo, G. Uncertainties in shoreline position analysis: The role of run-up and tide in a gentle slope beach. *Ocean Sci.* **2017**, *13*, 661–671. [\[CrossRef\]](#)
37. Fletcher, C.; Rooney, J.; Barbee, M.; Lim, S.C.; Richmond, B. Mapping shoreline change using digital orthophotogrammetry on Maui, Hawaii. *J. Coast. Res.* **2003**, *38*, 106–124.
38. Genz, A.S.; Fletcher, C.H.; Dunn, R.A.; Frazer, L.N.; Rooney, J.J. The predictive accuracy of shoreline change rate methods and alongshore beach variation on Maui, Hawaii. *J. Coast. Res.* **2007**, *23*, 87–105. [\[CrossRef\]](#)
39. Romine, B.M.; Fletcher, C.H.; Frazer, L.N.; Genz, A.S.; Barbee, M.M.; Lim, S.C. Historical shoreline change, southeast Oahu, Hawaii; applying polynomial models to calculate shoreline change rates. *J. Coast. Res.* **2009**, *25*, 1236–1253. [\[CrossRef\]](#)
40. Viridis, S.G.; Oggiano, G.; Disperati, L. A geomatics approach to multitemporal shoreline analysis in Western Mediterranean: The case of Platamona-Maritza beach (northwest Sardinia, Italy). *J. Coast. Res.* **2012**, *28*, 624–640.
41. Amore, C.; Randazzo, G. First data on the coastal dynamics and the sedimentary characteristics of the area influenced by the River Irminio basin (SE Sicily). *Catena* **1997**, *30*, 357–368. [\[CrossRef\]](#)
42. Pranzini, E. Pandemics and coastal erosion in Tuscany (Italy). *Ocean Coast. Manag.* **2021**, *208*, 105614. [\[CrossRef\]](#)
43. Zengcui, H.; Zeheng, D. Reclamation and river training in the Qiantang estuary. In *Engineered Coasts*; Chen, J., Eisma, D., Hotta, H.J., Walker, H.J., Eds.; Kluwer Academic Press: Dordrecht, The Netherlands, 2002; pp. 121–138.
44. Roskopf, C.M.; Di Paola, G.; Atkinson, D.E. Recent shoreline evolution and beach erosion along the central Adriatic coast of Italy: The case of Molise region. *J. Coast. Conserv.* **2018**, *22*, 879–895. [\[CrossRef\]](#)
45. Syvitski, J.P.; Vörösmarty, C.J.; Kettner, A.J.; Green, P. Impact of humans on the flux of terrestrial sediment to the global coastal ocean. *Science* **2005**, *308*, 376–380. [\[CrossRef\]](#)
46. Griggs, G.B. The impacts of coastal armoring. *Shore Beach* **2005**, *73*, 13–22.

47. Dugan, J.; Airolidi, L.; Chapman, M.; Walker, S.; Schlacher, T.; Wolanski, E.; McLusky, D. Estuarine and coastal structures: Environmental effects, a focus on shore and nearshore structures. In *Treatise on Estuarine and Coastal Science*; Wolanski, E., McLusky, D.S., Eds.; Academic Press: Waltham, MA, USA, 2011; Volume 8, pp. 17–41.
48. Hesp, P. Foredunes and blowouts: Initiation, geomorphology and dynamics. *Geomorphology* **2002**, *48*, 245–268. [\[CrossRef\]](#)
49. Scarelli, F.M.; Sistilli, F.; Fabbri, S.; Cantelli, L.; Barboza, E.G.; Gabbianelli, G. Seasonal Dune and beach monitoring using photogrammetry from UAV surveys to apply in the ICZM on the Ravenna coast (Emilia-Romagna, Italy). *Remote. Sens. Appl.* **2017**, *7*, 27–39. [\[CrossRef\]](#)
50. Díez-Garretas, B.; Comino, O.; Pereña, J.; Asensi, A. Spatio-temporal changes (1956–2013) of coastal ecosystems in Southern Iberian Peninsula (Spain). *Mediterr. Bot.* **2019**, *40*, 111–119. [\[CrossRef\]](#)
51. Carrasco, A.R.; Ferreira, O.; Matias, A.; Freire, P. Natural and human-induced coastal dynamics at back-back barrier beach. *Geomorphology* **2012**, *159–160*, 30–36. [\[CrossRef\]](#)
52. Psuty, N.P. Sediment budget and beach/dune interaction. *J. Coast. Res.* **1988**, *3*, 1–4.
53. Sherman, D.J.; Bauer, B.O. Dynamics of beach-dune interaction Progress. *Phys. Geogr.* **1993**, *17*, 413–447. [\[CrossRef\]](#)
54. Manno, G.; Ciraolo, G. Diachronic analysis of the shoreline in San Leone beach (Agrigento-Sicily). In *Establishment of an Integrated Italy-Malta Cross-Border System of Civil Protection—Geological Aspects*; Aracne: Catania, Italy, 2015.
55. Anfuso, G.; del Pozo, J.A.M. Towards management of coastal erosion problems and human structure impacts using GIS tools: Case study in Ragusa Province, Southern Sicily, Italy. *Environ. Geol.* **2005**, *48*, 646–659. [\[CrossRef\]](#)
56. Charlier, R.H.; Chaîneux, M.C.P.; Morcos, S. Panorama of the history of coastal protection. *J. Coast. Res.* **2005**, *21*, 79–111. [\[CrossRef\]](#)
57. Stancheva, M.; Marinski, J. Coastal defense activities along the Bulgarian Black Sea coast-methods for protection or degradation? In *Coastal Structures, Proceedings of the 5th International Conference, Venice, Italy, 2–4 July 2007*; Franco, L., Tomasicchio, G., Lamberti, A., Eds.; World Scientific Publishing Company: Singapore, 2007; pp. 480–489.
58. Stancheva, M. Human-induced impacts along the Coastal Zone of Bulgaria. A pressure boom versus environment. *Compt. Rend. Acad. Bulg. Sci.* **2007**, *63*, 137–146.
59. Manno, G.; Anfuso, G.; Messina, E.; Williams, A.T.; Suffo, M.; Liguori, V. Decadal evolution of coastline armouring along the Mediterranean Andalusia littoral (South of Spain). *Ocean Coast. Manag.* **2016**, *124*, 84–99. [\[CrossRef\]](#)
60. Anfuso, G.; Dominguez, L.; Gracia, F. Short and medium-term evolution of a coastal sector in Cadiz, SW Spain. *Catena* **2007**, *70*, 229–242. [\[CrossRef\]](#)
61. Sousa, P.; Siegle, E.; Tessler, M. Vulnerability assessment of Massaguaçu Beach (SE Brazil). *Ocean. Coast. Manag.* **2013**, *77*, 24–30. [\[CrossRef\]](#)
62. Sousa, P.; Siegle, E.; Tessler, M. Environmental and anthropogenic indicators for coastal risk assessment at Massaguaçu Beach (SP) Brazil. *J. Coast. Res.* **2011**, *64*, 319–323.
63. Oliver, T.; Tamura, T.; Short, A.; Woodroffe, C. Rapid shoreline progradation followed by vertical foredune building at Pedro Beach, southeastern Australia. *Earth Surf. Process. Landf.* **2018**, *44*, 655–666. [\[CrossRef\]](#)
64. Manca, E.; Pascucci, V.; Deluca, M.; Cossu, A.; Andreucci, S. Shoreline evolution related to coastal development of a managed beach in Alghero, Sardinia, Italy. *Ocean. Coast. Manag.* **2013**, *85*, 65–76. [\[CrossRef\]](#)
65. Saye, S.E.; Van der Wal, D.; Pye, K.; Blott, S.J. Beach—Dune morphological relationships and erosion/accretion: An investigation at five sites in England and Wales using LIDAR data. *Geomorphology* **2005**, *72*, 128–155. [\[CrossRef\]](#)